ICSV14

Cairns • Australia
9-12 July, 2007

14th
International Congress on
Sound &
Vibration

A SELECTIVE OVERVIEW OF HIGH-ORDER FINITE DIFFERENCE SCHEMES FOR AEROACOUSTIC APPLICATIONS

I. Spisso[1][*], A. Rona[1][†]

[1]Department of Engineering
University of Leicester
Leicester LE1 7RH, United Kingdom

[*]is71@le.ac.uk
[†]ar45@le.ac.uk

Abstract

A variety of aeroacoustic problems involve small-amplitude linear wave propagation. High-order schemes have the accuracy and the low dispersion and dissipation wave propagation properties that are required to model linear acoustic waves with minimal spatial resolution. This review presents a selection of high-order finite difference time-explicit schemes for aeroacoustic applications. A scheme selection method based on the computational cost for a given accuracy level is proposed.

1.   INTRODUCTION

The growing demand by aerospace, automotive and other industries for accurate and reliable noise prediction models has prompted the development of new computational aeroacoustic (CAA) methods. These are used not only as noise prediction tools, but also to evaluate new approaches for noise reduction and control. Different aeroacoustic problems often exhibit different flow physics. As a result, there is no single algorithm that can be used to simulate all problems with adequate resolution and accuracy. The quality of CAA predictions are affected by numerical dispersion and dissipation, the performance of acoustically transparent boundary conditions, the ability to simulate nonlinearities and to resolve disparate length scales [1, 2]. Any investigator developing a new CAA algorithm or applying an existing method must ensure that the method adequately addresses the above. Several CAA methods have emerged in last two decades [2, 3] and the progress on the state of art is documented in the proceedings of four CAA workshops on benchmark problems [4, 5, 6, 7].

This paper presents a compendium of the spatial discretization performance of selected CAA algorithms and gives a practical selection method to be used by the CAA predictioner for a given application, which accounts for the available computational resources.

2. SPATIAL DISCRETIZATION: NUMERICAL WAVENUMBER AND GROUP VELOCITY

A general approximation of the first derivative by a (M+N+1) point stencil at the x_i node of a uniform mesh with spacing Δx can be written as [1]

$$\sum_{j=-L}^{K} c_j \frac{\partial f}{\partial x}(x_i + j\Delta x) \approx \frac{1}{\Delta x} \sum_{j=-N}^{M} a_j f(x_i + j\Delta x) \tag{1}$$

where $L \leq N$ and $K \leq M$. The value of the coefficients c_j can be adjusted to achieve the desired order of accuracy and wave propagation performance. If $c_j = \delta_{ij}$, where δ_{ij} is the Kroneker delta, then the spatial approximation of equation (1) is explicit. If $c_j \neq 0$ for any $j \neq i$, equation (1) becomes implicit, or compact, and a matrix has to be inverted to determine the unknown values of $(\partial f/\partial x)_i$. Explicit schemes employ large computational stencils for a given accuracy, while compact schemes use smaller stencils by solving for the spatial derivatives as independent variables at each grid point. While compact schemes are more accurate than the same stencil size equivalent explicit schemes, they have two disadvantages: first, a matrix must be inverted to obtain the spatial derivative at each point; second, the boundary stencil has a large effect on the stability and accuracy of the scheme [8].

The coefficients a_j in an explicit finite-difference central scheme are typically obtained by truncation of a Taylor series. For a 7-point (ST7) and 9-point (ST9) stencil, a 6th and a 8th order accurate scheme are obtained respectively [9].

The application of the Fourier transform to the approximation of equation (1) with x_i replaced by a continuous variable x yields the effective wavenumber $\bar{\alpha}\Delta x$ of the finite-difference operator

$$\overline{\alpha}\Delta x = -i \left(\frac{\sum_{j=-L}^{K} a_j e^{ij\alpha\Delta x}}{\sum_{j=-N}^{M} c_j e^{ij\alpha\Delta x}} \right) \tag{2}$$

Figure 1 shows equation (2), plotted for different finite difference schemes over the non-dimensional wavenumber range $0 \leq \alpha\Delta x \leq \pi$. High order and optimized schemes can have a nearly exact differentiation down to 3 points per wavelength.

The group velocity of a finite-difference scheme is determined by $d\bar{\alpha}/d\alpha$ [10]. When $d\bar{\alpha}/d\alpha = 1$, the scheme has the same group velocity as the original governing equations and the numerical waves propagate at their correct wave speeds. The schemes becomes dispersive in the wavenumber range where $d\bar{\alpha}/d\alpha \neq 1$. If the right-hand side of equation (1) is a central difference ($M = N, a_j = a_{-j}, -N < j < N$) and the left-hand side is symmetric ($K = L, c_j = c_{-j}, -N < j < N$) then $\bar{\alpha}$ is real and the discretization of equation (1) is non-dissipative, that is, it does not generate any amplitude error [11].

In the next sections, the performance of the selected finite-difference schemes is reviewed based on the numerical wavenumber and numerical group velocity characteristics. The spatial operators examined here are a representative sample of those commonly used time-explicit finite-difference schemes.

2.1. Explicit central-difference DRP scheme

The DRP (Dispersion-Relation-Preserving) scheme of Tam and Webb [12, 11] is an explicit scheme with a seven-point central difference stencil,

$$\left(\frac{\partial f}{\partial x}\right)_i \approx \left(\frac{\sum_{j=1}^{3} a_j(f_{i+j} - f_{i-j})}{\Delta x}\right) \tag{3}$$

a_2 and a_3 are chosen so that equation (3) is accurate to the fourth order while a_1 is defined by an optimization parameter E to minimize the integrated error between $\bar{\alpha}\Delta x$ and $\alpha\Delta x$. Figure 1 shows that this results in an approximation with a better resolution of the high wavenumbers as compared to the formally higher order but unoptimized ST7 scheme.

Bogey and Baily [13], using the same theory as Tam, do not minimize the absolute difference between $\bar{\alpha}\Delta x$ and $\alpha\Delta x$ but their relative difference. The result is a 9-point, 4th order accurate scheme with a better high wavenumber performance than the standard ST9, as shown in figure 1.

The optimized operator of Zingg [14] is also a non-compact seven point stencil. The discretization is divided into a central-difference part approximating the derivative and a symmetric part providing artificial dissipation of spurious numerical waves [14].

2.2. Compact schemes

The optimized "spectral-like" compact scheme of Lele [9] is a pentadiagonal scheme with a seven-point stencil given by

$$\beta D_{i-2} + \eta D_{i-1} + D_i + \eta D_{i+1} + \beta D_{i+2} \approx c\frac{f_{i+3} - f_{i-3}}{\Delta x} + b\frac{f_{i+2} - f_{i-2}}{4\Delta x} + a\frac{f_{i+1} - f_{i-1}}{2\Delta x} \tag{4}$$

where D_i denotes the spatial derivative $(\partial f/\partial x)_i$ at the ith mesh node . The coefficients of the approximation are computed by Lele with three constrains imposed on the numerical wavenumber $\bar{\alpha}\Delta x$. This scheme is formally fourth-order accurate but has a significant wavenumber resolution performance. The optimized compact scheme of Lele exhibits the best wave propagation performance among the schemes in figure 1. It is capable of resolving very short waves; however this performance is achieved at the price of inverting a pentadiagonal matrix.

The work of Lele spawned an entire family of optimized compact schemes. Among these, the tridiagonal schemes with a five-point stencil obtained by setting $\beta = 0$ and $c = 0$ in equation (4) is particularly attractive because of the reduced cost of the matrix inversion [15]. Hixon [8, 16] derived a new class of compact schemes that obtain high-order accuracy while using an even shorter stencil. In Hixon's approach, the derivative operator D_i is split into a forward component, D_i^F, and backward component, D_i^B, so that $D_i = \frac{1}{2}(D_i^F + D_i^B)$. The compact discretization then becomes:

$$aD_{i+1}^F + (1 - a - c)D_i^F + cD_{i-1}^F \cong \frac{1}{\Delta x}[bf_{i+1} - (2b - 1)f_i - (1 - b)f_{i-1}] \qquad (5)$$

$$cD_{i+1}^B + (1 - a - c)D_i^B + aD_{i-1}^B \cong \frac{1}{\Delta x}[(1 - b)f_{i+1} + (2b - 1)f_i - bf_{i-1}] \qquad (6)$$

The coefficients of Hixon's six-order scheme are $a = \frac{1}{2} - \frac{1}{2\sqrt{5}}$, $b = 1 - \frac{1}{30a}$, $c = 0$. The stencil is reduced to three points and the tridiagonal matrix is replaced by two bidiagonal matrices.

Ashcroft and Zhang [17] attempted a wavenumber optimization that uses a Fourier analysis to determine the coefficients of the biased stencils. Figure 1 shows the $\bar{\alpha}\Delta x$ of the (6/4) optimized prefactored compact scheme of Ashcroft and Zhang. The first digit refers to the maximum order of accuracy of the scheme, while the second refers to actual order of the optimization. This scheme sacrifices the formal order of accuracy in favour of wide-band performance that provides significantly better wave propagation characteristics in the high wavenumber range ($-\circ$ line in figure 1) compared with the classical prefactorization of Hixon ($-*-$ line in the same figure). The dispersive charateristic of this scheme is shown figure 3; the scheme exhibits a low dispersion error for $\alpha\Delta x$ down to almost 1.4, where $\left|\frac{d\bar{\alpha}\Delta x}{d\alpha\Delta x} - 1\right| < 0.001$.

3. COMPARISONS IN WAVENUMBER SPACE

In Figure 1 it can be observed that $\bar{\alpha}\Delta x$ approximates adequately $\alpha\Delta x$ only over a limited range of long waves. For convenience, the maximum resolvable wavenumber will be denoted by $\bar{\alpha}_{nw}$. Using a criterion of $|\bar{\alpha}\Delta x - \alpha\Delta x| < 0.05$, a list of $\bar{\alpha}_{nw}\Delta x$ for the selected central difference schemes is given in table 1. The resolution of the spatial discretization, from $\bar{\alpha}_{nw}\Delta x$, is represented by the minimum points-per-wavenumber (Res. ppw) needed to reasonably resolve a propagating wave whose minimum is given by $(2\pi/\bar{\alpha}_{nw}\Delta x)$. An alternative criterion to determinate the resolution threshold $\bar{\alpha}_{pse}\Delta x$ is to impose that the phase speed error is $\left|\frac{d\bar{\alpha}\Delta x}{d\alpha\Delta x} - 1\right| < 0.001$. Table 1 present also the value of the stencil size (N_{st}) of each scheme, the maximum effective wavenumber $\bar{\alpha}_{max}\Delta x$, and the number of operation (adds + multiplies) for a single point spatial differentiation.

It is noted that at high frequencies ($\alpha\Delta x > 1.2$) $\bar{\alpha}$ begins to differ from α. An important consequence of this discrepancy is numerical dispersion. The short waves are highly dispersive and propagate with a phase speed quite different from the physical wave speed of the original partial differential equation. These short waves can cause spurious high-frequencies oscillations and can lead to instabilities [18]. Spurious waves can be generated by solutions discontinuities, solid surfaces, computational domain boundaries, grid interfaces and other irregularities. To improve the quality of the prediction these spurious waves are removed by filtering [14, 9, 10, 19, 20].

4. COMPUTATIONAL EFFICIENCY

Higher-order and optimized scheme achieve lower errors than low-order schemes for a given mesh size, but at an increased computational expense. Therefore, a method to select an appropriate scheme for a given application that requires a certain level of accuracy is sought [18]. Colonius and Lele [2] provide a single version of such a selection method that does not consider

the memory requirements and the parallelization efficiency. While the error in a solution may be measured in various ways (phase error, amplitude error, overall error from various norms), the method selector considers the error in the modified wavenumber, consistent with previous work [2]. The wavenumber is proportional to the minimum number of point per wavelength Res (ppw). When scaled with the computational cost per node, ppw is a measure of the total "cost"of computing a spatial derivative for a particular wavelength. The computational total cost of computing once the spatial gradients of a wave of wavenumber α to a given level of accuracy is given by $C \propto N_{op}ppw^2\bar{\alpha}_{max}\Delta x$, where ppw is the number of point per wavelenght used to resolve α.

In figure 4 it is shown the error in the modified wavenumber versus the estimated cost of the schemes examined. Using figure 4, it is possible to ascertain which scheme has the lowest error for a given cost, and how many grid points per wavelength should be used with that scheme to achieve that accuracy. Also, for a given error tolerance, the plot shows which scheme has the lowest cost. For example, for a normalized cost of 2, the lowest error (around 0.1%) is obtained with the optimized prefactored compact schemes of Ashcroft and Zhang, which has a slightly better performance than the prefactored sixth order scheme of Hixon. For the same cost the two schemes have the same minimum number of points per wavelenght (≈ 3) but Hixon's scheme has globally a lower phase speed error.

5. CONCLUSION

This paper examined a selection of high-order finite-difference algorithms for CAA and reviewed their main characteristics. A scheme selection method, based on the computational cost for a given accuracy level, was proposed, following the work of Colonius [2]. It is concluded that the combination of the filtered sixth order compact scheme of Hixon [8] with the 4-6 alternate Low Dispersion and Dissipation Runge-Kutta (LDDRK) [16, 21, 22] scheme is a good starting choice for aeroacoustic problems in the near-incompressible regime, as it gives the best compromise between computational cost and a dispersion and dissipation error.

6. ACKNOWLEDGMENT

Table 1. Properties of the schemes.

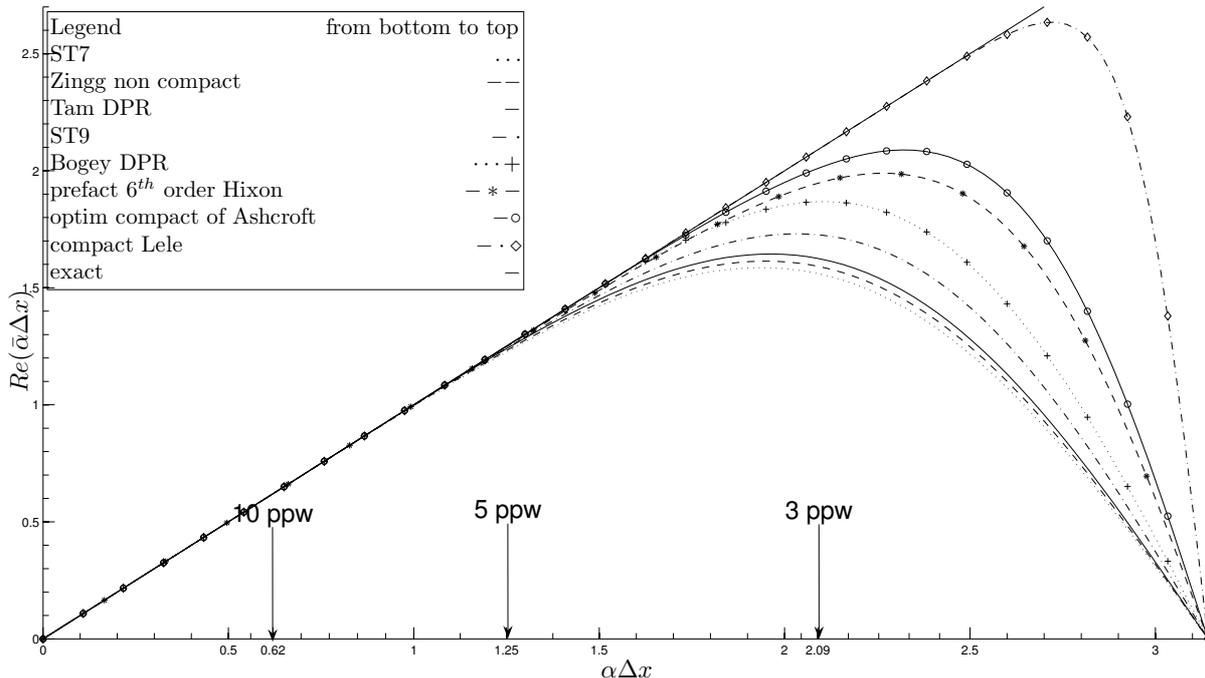| Spatial Discretization	N_{st}	N_{op}	$\bar{\alpha}_{max}\Delta x$	$\bar{\alpha}_{nw}\Delta x$	Res. (ppw)	$\bar{\alpha}_{pse}\Delta x$	Res.(ppw)
ST7	7	8	1.59	0.97	6.5	0.53	11.8
ST9	9	11	1.73	1.18	5.3	0.73	8.6
Tam DPR	7	8	1.64	1.16	5.4	0.43	14.6
Bo. and Ba. DPR	9	11	1.86	1.54	4.1	0.5	12.5
Zingg non-compact	7	18	1.61	1.05	5.9	0.66	9.52
compact Lele	7	17	2.63	2.51	2.5	0.94	6.68
compact Hixon	5	9	1.99	1.35	4.6	0.8	7.85
opt. precomp. Ashcroft	5	9	2.09	1.66	3.8	0.67	9.37

Figure 1. Dispersive characteristics of eight finite-difference schemes. Real part of numerical wavenumber versus exact wavenumber.
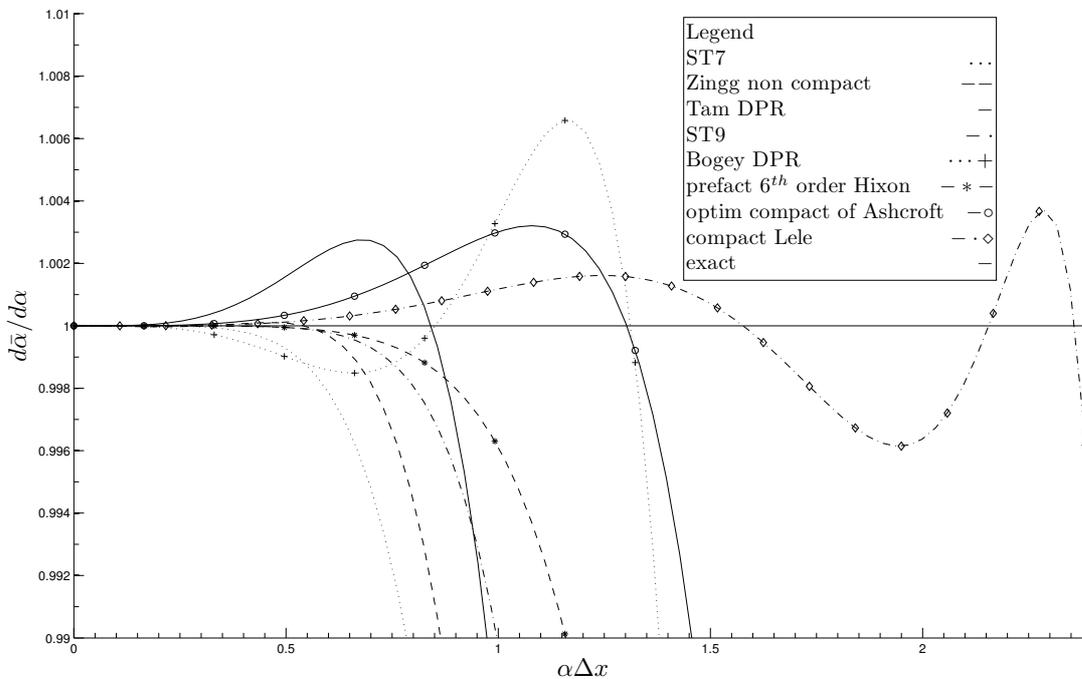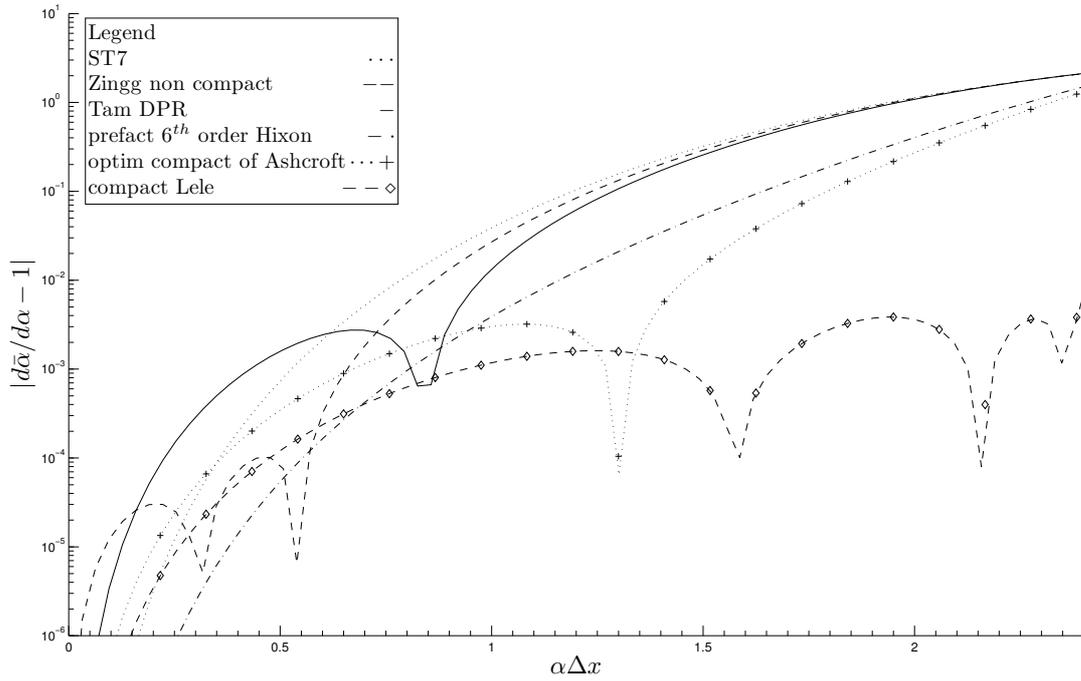

Figure 2. Non dimensional group velocity.
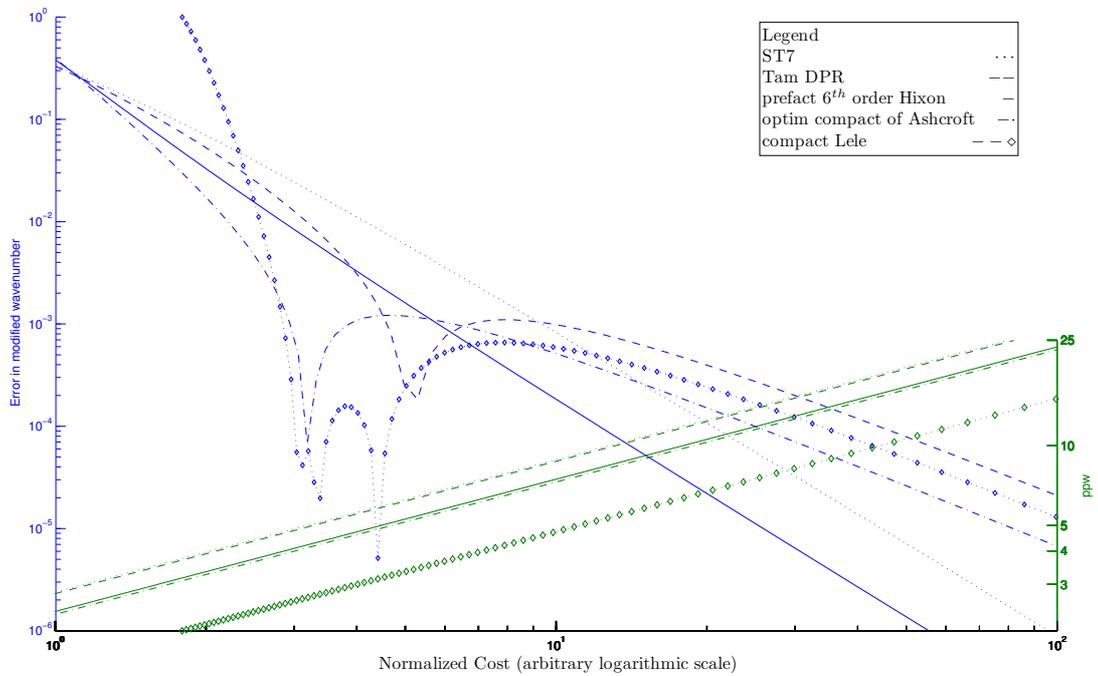
Figure 3. Phase speed error.

Figure 4. Computational efficiency.

REFERENCES

[1] K. Kurbatskii and R. Mankbadi, "Review of computational aeroacoustics algorithms," *Int. J. Computational Fluid Dynamics*, vol. 18, no. 6, pp. 533–46, 2004.

[2] T. Colonius and S. Lele, "Computational aeroacoustics: progress on nonlinear problems of sound generation," *Progress on Aerospace Sciences*, vol. 40, no. 6, pp. 345–416, 2004.

[3] W. D. Roeck, W. Desmet, M. Baelmans, and P. Sas, "An overview of high-order finite difference schemes for computational aeroacoustics," in *International Conference on Noise and Vibration Engineering*. ISMA, 2004, pp. 353–368.

[4] J. Hardin, J. R. Ristorcelli, and C. Tam, Eds., *Workshop on Benchmark Problems in Computational Aeroacoustics (CAA)*. Hampton, Va: NASA Conference Publication 3300, October 1995.

[5] J. Hardin and C. Tam, Eds., *Second Computational Aeroacoustics (CAA) Workshop on Benchmark Problems proceedings of a workshop*. Hampton, Va: NASA Conference Publication 3352, November 1997.

[6] J. Hardin, D. Huff, and C. Tam, Eds., *Third Computational Aeroacoustics (CAA) Workshop on Benchmark Problems*. Cleveland, Ohio: NASA Conference Publication 2000-209790, August 2000.

[7] M. Dahl, E. Envia, D. Huff, and C. Tam, Eds., *Fourth Computational Aeroacoustics (CAA) Workshop on benchamrck problems*. Brook Park, Ohio: NASA Conference Publication 2004-212954, October 2003.

[8] R. Hixon, "A new class of compact schemes," 37th Aerospace Sciences Meeting and Exhibit, Reno, NV, Tech. Rep. AIAA 98-0367, January 1998.

[9] S. K. Lele, "Compact finite difference schemes with spectral-like resolution," *Journal of Computational Physics*, vol. 103, no. 1, pp. 16–42, 1992.

[10] C. Tam and H. N. Shen, "Direct computation of nonlinear acoustic pulses using high-order finite difference schemes," *AIAA Journal*, vol. 93, no. (3382), 1993.

[11] C. Tam, "Computational aeroacoustics: Issues and methods," Tech. Rep. AIAA 1995-0677, 1995.

[12] C. K. W. Tam and J. C. Web, "Dispersion-relation-preserving finite difference schemes for computational acoustics," *Journal of Computational Physics*, vol. 107, pp. 262–281, 1993.

[13] C. Bogey and C. Bailly, "A family of low dispersive and low dissipative explicit schemes for flow and noise computations," *Journal of Computational Physics*, vol. 194, no. 1, pp. 194–214, 2004.

[14] D. W. Zingg, H. Lomax, and H. Jurgens, "High-accuracy finite-difference schemes for linear wave propagation," *SIAM Journal of Scientific Computing*, vol. 17, no. 2, pp. 328–346, 1996.

[15] Z. Haras, "Finite difference schemes for long-time integration," *Journal of Computational Physics*, vol. 114, no. 2, pp. 265–279, 1994.

[16] R. Hixon, "Prefactored small-stencil compact schemes," *Journal of Computational Physics*, vol. 165, no. 2, pp. 522–41, 2000.

[17] G. Ashcroft and X. Zhang, "Optimized prefactored compact schemes," *Journal of Computational Physics*, vol. 190, no. 2, pp. 459–477, 2003.

[18] T. Colonius, "Computational aeroacoustics," in *Lecture Series*. Rhode Saint Genése Belgium: Von Karman Institute for Fluid Dynamics, 2006.

[19] C. Kennedy and M. Carpenter, "Several new numerical methods for compressible shear-layer simulations," *Appl. Num. Math*, vol. 14, pp. 397–433, 1994.

[20] C. Tam, J. Webb, and Z. Dong, "A study of the short wave components in computational acoustics," *J. Comp. Acoust*, vol. 1, pp. 1–30, 1993.

[21] F. Hu, M. Hussaini, and J. Manthey, "Low-dissipation and low-dispersion Runge-Kutta schemes for computational acoustics," *J. Computational Physics*, vol. 124, pp. 177–191, 1996.

[22] R. Hixon, "On increasing the accuracy of MacCormack schemes for aeroacoustic applications," NASA, Contract Report 202311 ICOMP-96-11, December 1996.